Space radiation triggers persistent stress response, increases senescent signaling, and decreases cell migration in mouse intestine

Santosh Kumar[a,b,1], Shubhankar Suman[a,b,1], Albert J. Fornace Jr.[a,b], and Kamal Datta[a,b,2]

[a]Department of Biochemistry and Molecular and Cellular Biology, Georgetown University, Washington, DC 20057; and [b]Lombardi Comprehensive Cancer Center, Georgetown University, Washington, DC 20057

Edited by James E. Cleaver, University of California, San Francisco, CA, and approved August 30, 2018 (received for review May 1, 2018)

Proliferative gastrointestinal (GI) tissue is radiation-sensitive, and heavy-ion space radiation with its high-linear energy transfer (high-LET) and higher damaging potential than low-LET γ-rays is predicted to compromise astronauts' GI function. However, much uncertainty remains in our understanding of how heavy ions affect coordinated epithelial cell migration and extrusion, which are essential for GI homeostasis. Here we show using mouse small intestine as a model and BrdU pulse labeling that cell migration along the crypt–villus axis is persistently decreased after a low dose of heavy-ion ^{56}Fe radiation relative to control and γ-rays. Wnt/β-catenin and its downstream EphrinB/EphB signaling are key to intestinal epithelial cell (IEC) proliferation and positioning during migration, and both are up-regulated after ^{56}Fe radiation. Conversely, factors involved in cell polarity and adhesion and cell–extracellular matrix interactions were persistently down-regulated after ^{56}Fe irradiation—potentially altering cytoskeletal remodeling and cell extrusion. ^{56}Fe radiation triggered a time-dependent increase in γH2AX foci and senescent cells but without a noticeable increase in apoptosis. Some senescent cells acquired the senescence-associated secretory phenotype, and this was accompanied by increased IEC proliferation, implying a role for progrowth inflammatory factors. Collectively, this study demonstrates a unique phenomenon of heavy-ion radiation-induced persistently delayed IEC migration involving chronic sublethal genotoxic and oncogenic stress-induced altered cytoskeletal dynamics, which were seen even a year later. When considered along with changes in barrier function and nutrient absorption factors as well as increased intestinal tumorigenesis, our in vivo data raise a serious concern for long-duration deep-space manned missions.

intestinal epithelial cell migration | cytoskeleton remodeling | DNA damage | senescence | SASP

Ionizing radiation (IR) exposure as a risk factor for chronic gastrointestinal (GI) pathologies including colorectal cancer has been reported in atom bomb survivors and radiological workers (1–3). Increasing interest in human exploration of outer space is fraught with exposure to IR, which is considerably different from radiation on Earth. Astronauts traveling on long-duration space missions, such as missions to Mars, will be exposed to energetic particle radiation, including protons and heavy ions from solar particle events and galactic cosmic radiation (4, 5). While protons are the major component of space radiation, energetic heavy ions such as ^{56}Fe, ^{28}Si, and ^{12}C contribute significantly toward the dose equivalent, and ∼30% of astronauts' cells are predicted to be hit by heavy ions during a round trip to Mars (6, 7). For NASA mission planners, heavy ions are of major concern because they are difficult to block with current shielding measures. Also, qualitatively heavy ions are high-linear energy transfer (high-LET) and densely ionizing, and deposit higher focal energy in traversed tissues relative to terrestrial low-LET sparsely ionizing γ-rays or X-rays (5). Importantly, heavy ions, such as ^{12}C, with its higher relative biological effectiveness and better dose distribution relative to photon-based radiotherapy, are increasingly used for overcoming radioresistance and extending cancer patients' survival (8). The GI tract with its high cell turnover is sensitive to radiation, and the effects of radiation are evident when the replacement process of cells lost during normal turnover is deregulated. In the small intestine, considered a model system to study GI epithelial cell turnover (9), differentiated epithelial cells from crypt-base stem cells migrate along the crypt–villus axis to replace cells that shed into intestinal lumen via apoptosis at the villus tip (10). While heavy ions are predicted to pose greater risk to GI tissue homeostasis, at present there is much uncertainty in understanding heavy-ion radiation-related GI risk because sufficient in vivo mechanistic data are not available. We previously demonstrated differential long-term stress responses after heavy ions compared to γ-rays in intestinal epithelial cells (IECs) (4). However, it remains to be elucidated how heavy ions modulate molecular events associated with IEC migration, which is essential for maintaining physiological integrity such as nutrient absorption and barrier function and preventing pathological processes such as inflammatory or malabsorption disorders, as well as GI cancer.

Migration of IECs is a bidirectional phenomenon, with all of the differentiated cells moving toward the lumen except Paneth cells, which move toward the crypt base. IEC migration is tightly regulated to minimize exposure time to physical and biochemical insults from luminal contents while maintaining optimal cell turnover for functional integrity (11). Wnt signaling plays key roles in maintaining intestinal cell turnover homeostasis and coordinates with other signaling pathways to regulate proliferation, differentiation, migration, and shedding of IECs (12). Furthermore, Dickkopf-1

Significance

Coordinated epithelial cell migration is key to maintaining functional integrity and preventing pathological processes in gastrointestinal tissue, and is essential for astronauts' health and space mission success. Here we show that energetic heavy ions, which are more prevalent in deep space relative to low-Earth orbit, could persistently decrease intestinal epithelial cell migration, alter cytoskeletal remodeling, and increase cell proliferation with ongoing DNA damage and cell senescence, even a year after irradiation. Our study has provided the molecular underpinnings for energetic heavy-ion ^{56}Fe radiation-induced cell migration alterations, and raises a potentially serious concern, particularly for long-term deep-space manned missions.

Author contributions: S.K., S.S., and K.D. designed research; S.K. and S.S. performed research; S.K., S.S., and K.D. analyzed data; and S.K., S.S., A.J.F., and K.D. wrote the paper.

The authors declare no conflict of interest.

This article is a PNAS Direct Submission.

[1]S.K. and S.S. contributed equally to this work.

[2]To whom correspondence should be addressed. Email: kd257@georgetown.edu.

This article contains supporting information online at www.pnas.org/lookup/suppl/doi:10.1073/pnas.1807522115/-/DCSupplemental.

Published online October 1, 2018.

(Dkk1), a Wnt antagonist, has been reported to attenuate directional polarization and migration of IECs (13). Importantly, the Wnt-signaling downstream effector β-catenin ensures compartmentalization of IECs in crypts and villi through transcriptional regulation of EphB/EphrinB signaling (12). Furthermore, increased transgenic expression of β-catenin has been reported to cause increased DNA damage and γH2AX foci, and activation of the DNA damage response possibly due to oncogenic stress (14). Increased DNA damage could also be induced by chronic oxidative stress, which has been reported to activate β-catenin (15). DNA damage has been reported to adversely impact the cytoskeleton (16), and efficient cytoskeletal remodeling is essential for coordinated migration of IECs along the crypt–villus axis through regulation of cell polarity, tight junction, adhesion, actomyosin, and microtubule dynamics. Movement of IECs along the crypt–villus axis also requires interaction between epithelial cells and the extracellular matrix (ECM) via integrins (17). Integrins have been reported to modulate the DNA damage response, and activation of β1-integrin decreased DNA damage-induced apoptosis (16). Migrating IECs are shed at the villus tip via apoptosis, and the actin-binding protein villin, through its differential cleavage and interaction with actin, has been shown to regulate cell turnover in the villi (18). While heavy-ion radiation is capable of inducing long-lasting cellular stress and DNA damage (4, 19), its effects on key cellular processes involved in IEC migration and pathological implications of their dysregulation on GI tissue are poorly defined.

The current study now demonstrates that IEC migration along the crypt–villus axis is decreased after a low dose of heavy-ion radiation relative to γ-rays. While heavy ions activated β-catenin and EphB/EphrinB signaling, promoted cell proliferation, and increased the number of crypts, it also induced chronic oxidative stress and DNA damage without increasing cell death up to 12 mo after ^{56}Fe radiation. These effects correlated with higher levels of senescent cells in GI crypts and features of the senescence-associated secretory phenotype (SASP). Heavy-ion radiation induced long-term downregulation of factors involved in cytoskeletal remodeling, cell adhesion, cellular tight junction, and microtubule dynamics without altering the direction of cell migration. Overall, our study systematically analyzed and identified differential molecular perturbations underlying heavy ion- and γ-ray–induced decreased IEC migration that could aid in developing not only risk prediction models but also risk mitigation strategies for GI tissue in astronauts and patients.

Results

Decreased Rate of IEC Migration After Heavy-Ion Radiation Exposure. Our previous reports showed that exposure to ^{56}Fe radiation was associated with long-term adverse sequelae in the intestine of wild-type C57BL/6J as well as APC mutant ($APC^{Min/+}$ and $APC^{1638N/+}$) mice (4, 5). Some of our initial studies carried out at higher doses (>1 Gy) demonstrated a modest increase in lethality with 50% survival at 30 d ($LD_{50/30}$) for 5.8 Gy of ^{56}Fe ions compared to 7.25 Gy of γ-rays (20). However, our later studies at lower doses (<1 Gy) showed significantly higher intestinal tumorigenesis after heavy ions relative to γ-rays (5). Since the estimated radiation dose for a 1,000-d Mars mission is about 0.42 Gy (21), with an estimate of an 860-d Mars mission dose equivalent of ∼1.01 Sv (22) so doses of 0.5 Gy or less are more relevant, we have used 0.5 Gy to study IEC migration, which is important for intestinal homeostasis. We performed BrdU pulse labeling to assess the effects of low-dose γ- or ^{56}Fe irradiation on IEC migration along the crypt–villus axis in mouse small intestine. Exposure to ^{56}Fe radiation decreased cell migration 7 as well as 60 d after exposure, and that migration was significantly slower relative to control as well as γ-rays (Fig. 1 *A* and *B*). Quantification of migration distance in terms of cell number between the highest cell stained BrdU-positive and the lowest cell in the crypt showed a significant decrease in cell migration distance at both time points after ^{56}Fe relative to control and γ-rays (Fig. 1*C*). While cell migration was decreased 7 d after γ-rays relative to control, it was similar to control 60 d after γ-rays (Fig. 1*C*), suggesting recovery in γ-irradiated mice. For heavy ions, although IEC migration was higher after 60 d relative to 7 d, it was significantly lower at both time points relative to control and γ-rays, indicating longer persistence of ^{56}Fe-induced effects relative to γ-rays.

Heavy-Ion Radiation Activates Wnt/β-Catenin and Downstream Signaling in Mouse Intestine. To elucidate molecular events involved in the heavy-ion radiation-induced decreased cell migration, we examined the canonical Wnt/β-catenin pathway and its regulators due to its roles in cell proliferation, differentiation, and migration. While the Wnt antagonist Dkk-1 was decreased, active β-catenin was increased 7 (Fig. 2*A* and *SI Appendix*, Fig. S1*A*, *Left*) as well as 60 (Fig. 2*A* and *SI Appendix*, Fig. S1*A*, *Right*) d after ^{56}Fe radiation relative to control and γ-rays. Importantly, ^{56}Fe exposure led to increased phospho-GSK3β (Fig. 2*A* and *SI Appendix*, Fig. S1*A*), a GSK3β-inactivating event, supporting β-catenin accumulation at both time points. Because

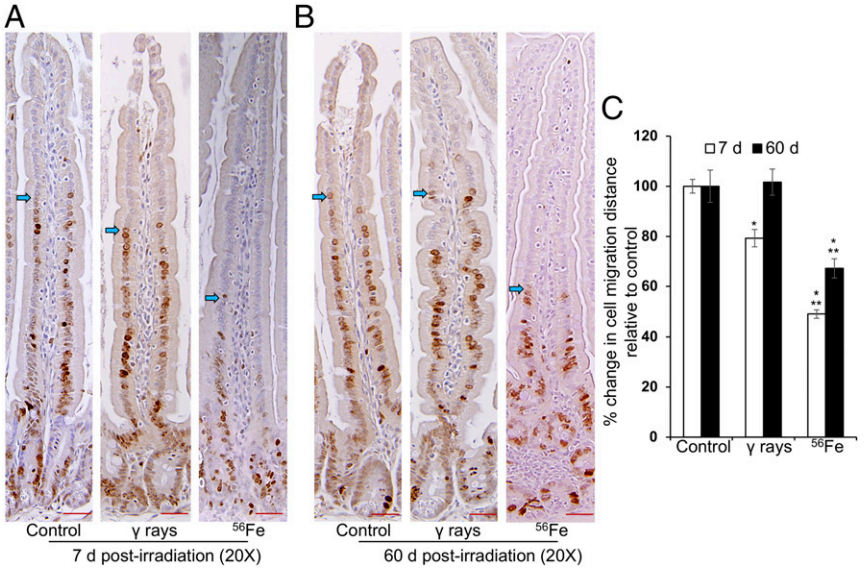

Fig. 1. Long-term decrease of IEC migration after ^{56}Fe radiation relative to γ-rays. (*A* and *B*) Sections of the jejunal–ilial region of mouse intestine 7 and 60 d after sham, γ-, or ^{56}Fe radiation exposure were immunohistochemically stained for BrdU 24 h after an i.p. BrdU injection and nuclei were counterstained with hematoxylin; a representative image from each group is presented showing slower IEC migration after ^{56}Fe radiation. (Scale bars, 10 μm.) (*C*) IEC migration distance was measured by counting the number of cells between the BrdU-stained top-most cell in the villus and the bottom-most cell in the crypt in 7- and 60-d postexposure samples; *, significant relative to control; **, significant relative to γ-rays. Arrows show cell migration height as well as highest labeled cell. Statistical significance is set at $P < 0.05$ and error bars represent mean ± SEM.

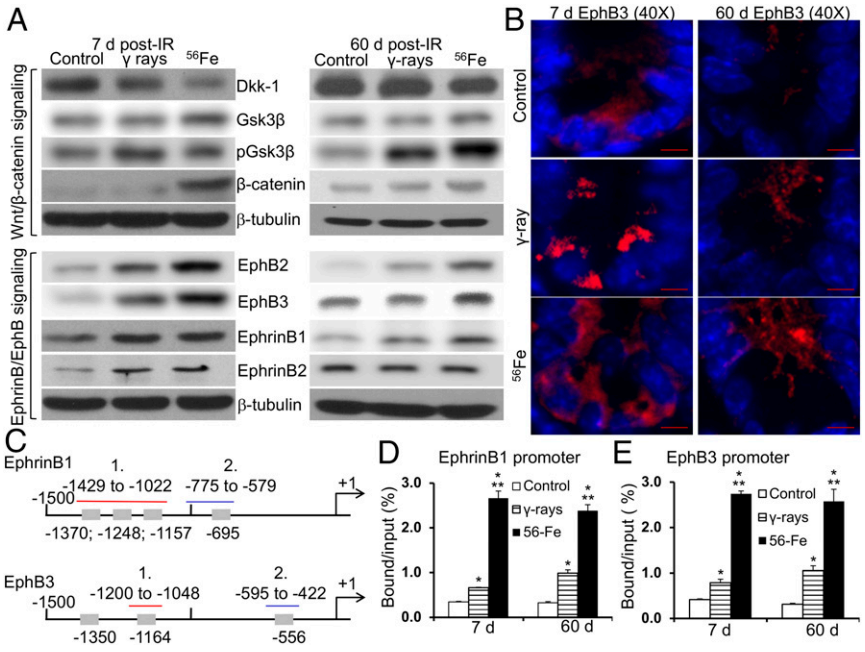

Fig. 2. Dysregulation of Wnt/β-catenin and EphB/EphrinB signaling after ^{56}Fe radiation. (*A*) Immunoblots show decreased Wnt antagonist Dkk1, increased phospho-GSK3β, increased activated β-catenin, and increased EphB/EphrinB after ^{56}Fe. (*B*) Immunofluorescence image showing increased EphB3 after ^{56}Fe radiation. (Scale bars, 5 μm.) (*C*) Putative TCF/LEF family of transcription factor binding sites on the promoter of the *EphrinB1* and *EphB3* genes relative to transcription start sites. While four binding sites are on the *EphrinB1* promoter, three binding sites are on the *EphB3* promoter. Gray boxes, binding sites; numbers, location of the binding-site end positions; colored lines and the numbers above, PCR primer span and the number of primer pairs; red lines, PCR nonamplification; blue lines, successful PCR amplification. (*D*) Quantitative RT-PCR results from immunoprecipitated DNA show enhanced β-catenin binding to the *EphrinB1* promoter after ^{56}Fe radiation. (*E*) qRT-PCR results showing enhanced β-catenin binding to the *EphB3* promoter after ^{56}Fe radiation; *, significant relative to control; **, significant relative to γ-rays. Statistical significance is set at $P < 0.05$ and error bars represent mean ± SEM.

β-catenin/TCF4 regulates expression of EphB (receptors) and EphrinB (ligands) and both are involved in IEC migration, the effects of ^{56}Fe radiation on EphB/EphrinB signaling were explored. Immunoblot analysis of EphB2 and EphB3 in irradiated samples from 7- and 60-d time points show enhanced expression after ^{56}Fe radiation relative to control and γ-rays (Fig. 2*A* and *SI Appendix*, Fig. S1*B*). EphrinB data show radiation-induced increased expression of EphrinB1 and EphrinB2 at 7- (Fig. 2*A* and *SI Appendix*, Fig. S1*B*, *Left*) as well as 60- (Fig. 2*A* and *SI Appendix*, Fig. S1*B*, *Right*) d time points. While EphrinB1 expression was similar after 7 d, it was higher after 60 d of ^{56}Fe irradiation relative to γ-rays (Fig. 2*A* and *SI Appendix*, Fig. S1*B*). Immunoblot data on EphrinB2 did not show any difference between the two radiation types (Fig. 2*A* and *SI Appendix*, Fig. S1*B*). Further validation of the EphB3 immunoblot data by immunofluorescence showed enhanced expression at 7 (Fig. 2*B* and *SI Appendix*, Fig. S1*C*, *Left*) and 60 (Fig. 2*B* and *SI Appendix*, Fig. S1*C*, *Right*) d after ^{56}Fe as well as after γ-radiation. However, expression of EphB3 was higher 60 d after ^{56}Fe relative to γ-rays (Fig. 2*B* and *SI Appendix*, Fig. S1*C*), suggesting differential effects of the two radiation types.

Enhanced β-Catenin/TCF4 Binding to *EphB3* and *EphrinB1* Promoters After ^{56}Fe Radiation Exposure. β-Catenin/TCF4 binds to TCF/LEF-binding elements on promoters of *EphrinB1* and *EphB3* genes. Putative TCF/LEF binding sites on *EphrinB1* and *EphB3* promoters were analyzed in silico (*SI Appendix*, Section *D*); results are presented schematically in Fig. 2*C*, and binding-site sequences are presented in *SI Appendix*, Tables S1 (*EphrinB1*) and S2 (*EphB3*). For *EphrinB1*, primer pair no. 1 (Fig. 2*C* and *SI Appendix*, Table S3) amplifies a region that covers three binding sites, which are contiguous, and primer pair no. 2 (Fig. 2*C* and *SI Appendix*, Table S3) covers the fourth binding site. For *EphB3*, primer pair no. 1 (Fig. 2*C* and *SI Appendix*, Table S3) covers the second binding site and primer pair no. 2 (Fig. 2*C* and *SI Appendix*, Table S3) covers the third binding site. For both *EphrinB1* and *EphB3* promoters, primer pair no. 1 (colored red, Fig. 2*C*) did not amplify the target sequence, suggesting lack of β-catenin/TCF4-bound DNA. Real-time PCR results from primer pair no. 2 (colored in blue, Fig. 2*C*) for β-catenin/TCF4-bound DNA of *EphrinB1* and *EphB3* promoters after radiation exposure are presented as percent input (Fig. 2 *D* and *E*). The result showed greater binding of β-catenin/TCF4 to the *EphrinB1* (Fig. 2*D*) and *EphB3* (Fig. 2*E*) promoters in irradiated groups at both time points. Higher *EphrinB1* and *EphB3* promoter enrichment was observed in the ^{56}Fe-irradiated group relative to the γ-irradiated group (Fig. 2 *D* and *E*), supporting the notion that heavy-ion radiation-induced increased β-catenin is translocating to the nucleus and participating in increased expression of *EphrinB1* and *EphB3*.

Radiation Attenuates Expression of Cell Polarity, Cytoskeleton, and Cell Adhesion Factors. We examined effects of ^{56}Fe radiation on expression of factors involved in regulating the cytoskeleton, cell polarity, and cell adhesion. While levels of Cdc42, myosin light-chain kinase (Mlck), Par3, and E-cadherin were decreased, expression of Rho-associated protein kinase 1 (Rock1) was increased 7 (Fig. 3*A* and *SI Appendix*, Fig. S2*A*, *Left*) and 60 (Fig. 3*A* and *SI Appendix*, Fig. S2*A*, *Right*) d after ^{56}Fe relative to control and γ-rays. Immunofluorescence staining for the cell polarity protein Par3 (Fig. 3*B* and *SI Appendix*, Fig. S2*B*, 7 d, *Left* and 60 d, *Right*) and cell adhesion protein E-cadherin (Fig. 3*C* and *SI Appendix*, Fig. S2*C*, 7 d, *Left* and 60 d, *Right*) demonstrates decreased staining in ^{56}Fe-irradiated samples relative to control and γ-rays. While decreased expression of Cdc42 and Mlck and increased Rock1 are expected to affect cytoskeletal remodeling, decreased levels of Par3 will alter cell polarity dynamics, impacting coordinated movement of cells. Decreased E-cadherin could not only contribute to decreased cell migration but could also affect the E-cadherin/β-catenin pool in favor of increased cytoplasmic β-catenin and thus increased availability for nuclear translocation.

Effects of Radiation on Tight Junction Proteins Are More Pronounced After ^{56}Fe Relative to γ-Rays. IEC migration occurs as a sheet of epithelial cells, and cellular tight junction (TJ) proteins play important roles in the dynamics of the epithelial cell sheet. Our data show greater decrease in Claudin1 and Zonula occludens-1 (Zo-1) levels in the ^{56}Fe-irradiated samples relative to γ-rays and control at 7 (Fig. 4*A* and *SI Appendix*, Fig. S3*A*, *Left*) as well as 60 (Fig. 4*A* and *SI Appendix*, Fig. S3*A*, *Right*) d after exposure. We also assessed effects of ^{56}Fe radiation on Zo-1, a scaffold protein connecting TJ transmembrane proteins and the actin cytoskeleton, in intestinal epithelium using immunofluorescence. We show that Zo-1 is decreased 7 (Fig. 4*B* and *SI Appendix*, Fig. S3*B*, *Left*) and 60 (Fig. 4*B* and *SI Appendix*, Fig. S3*B*, *Right*) d after

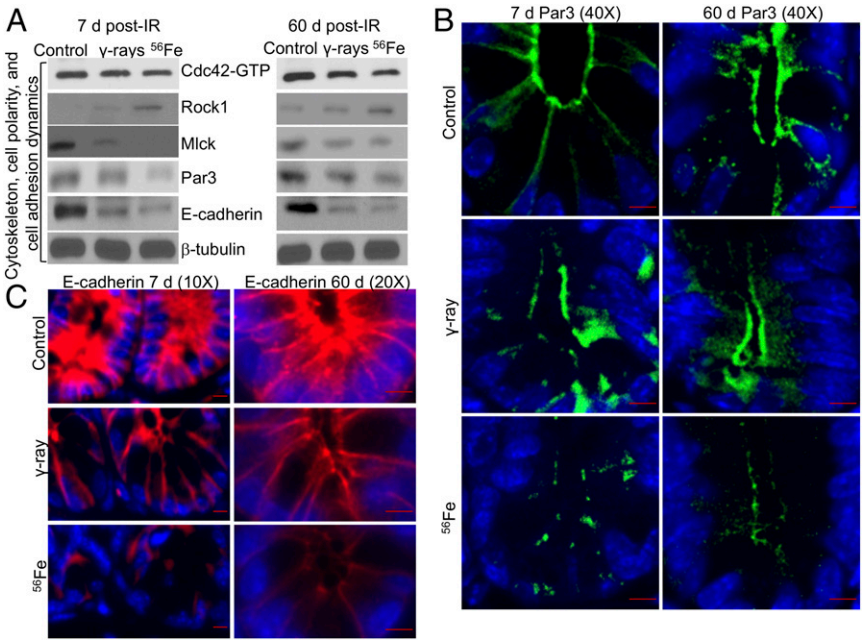

Fig. 3. Decreased cell polarity and adhesion protein expression after ^{56}Fe radiation. (*A*) Representative immunoblot images showing altered expression of factors involved in cytoskeleton (Cdc42, Rock1, Mlck), cell polarity (Par3), and cell adhesion (E-cadherin) dynamics 7 (*Left*) and 60 (*Right*) d after ^{56}Fe irradiation relative to γ-rays. (*B*) Intestinal sections were stained using anti-Par3 antibody, and representative images are presented showing decreased Par3 expression after ^{56}Fe radiation. (Scale bars, 5 μm.) (*C*) Intestinal sections stained for the cell adhesion marker E-cadherin, and representative images are presented showing decreased E-cadherin after ^{56}Fe radiation. (Scale bars, 10 μm.)

^{56}Fe radiation relative to γ-rays and control, thus supporting the immunoblot results. However, Occludin was unaltered in irradiated samples at both time points (Fig. 4*A* and *SI Appendix*, Fig. S3*A*). Additionally, Scrib, another key TJ protein, while showing a similar decrease after γ-rays and ^{56}Fe radiation at 7 d, was markedly lower after ^{56}Fe relative to γ-rays in 60-d postradiation samples (Fig. 4*A* and *SI Appendix*, Fig. S3*A*). Immunofluorescence staining for Scrib showed decreased staining in 7 (Fig. 4*C* and *SI Appendix*, Fig. S3*C*, *Left*) and 60 (Fig. 4*C* and *SI Appendix*, Fig. S3*C*, *Right*) d post–^{56}Fe-irradiated samples relative to control and γ-rays. Overall, our data suggest that decreased levels of TJ proteins are deregulating cell–cell interaction dynamics that could contribute to decreased cell migration.

Exposure to Heavy-Ion Radiation Altered Microtubule Dynamics but Did Not Alter Direction of Cell Migration. Microtubule-associated proteins (MAPs) play important roles in stabilizing assembled microtubules and thus regulating cellular motility. Our data on Map1b, Tau, and phospho-Tau showed levels of these MAPs involved in stabilizing microtubules are decreased 7 (Fig. 4*D* and *SI Appendix*, Fig. S4*A*, *Left*) and 60 (Fig. 4*D* and *SI Appendix*, Fig. S4*A*, *Right*) d after ^{56}Fe radiation, and decreases were greater relative to control and γ-rays. The Collapsin response mediator protein 2 (Crmp2) is a non-MAP protein that has been reported to regulate microtubule dynamics (23). Our data show that Crmp2 level, though unaltered at 7 d, was decreased at 60 d after ^{56}Fe radiation exposure relative to control and γ-rays (Fig. 4*D* and *SI Appendix*, Fig. S4*A*), suggesting long-term effects of heavy-ion radiation on microtubule dynamics and thus on cell

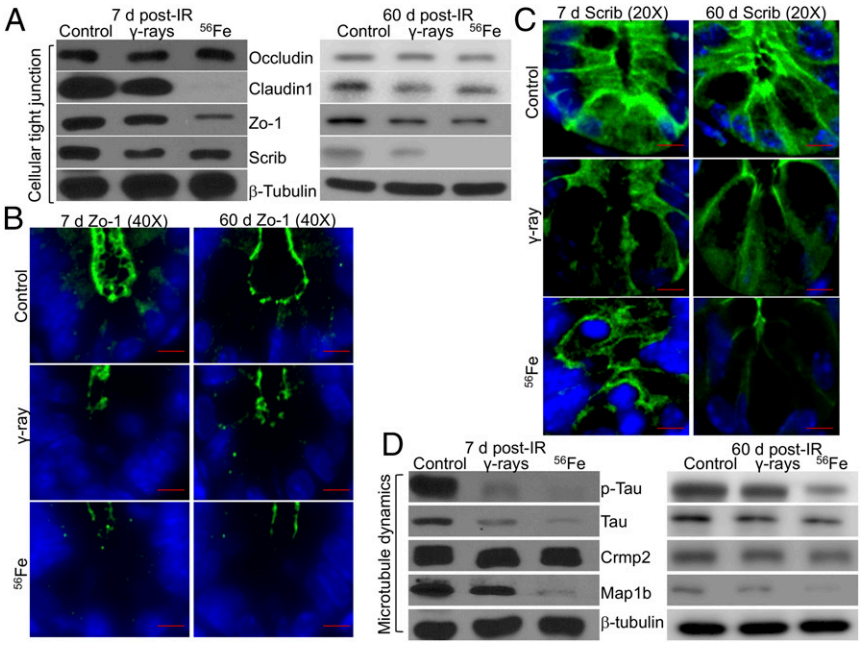

Fig. 4. Heavy-ion radiation decreases expression of key cellular tight junction proteins and alters microtubule dynamics in mouse intestine. (*A*) Representative immunoblot images of cellular tight junction proteins showing radiation-induced altered expression of Occludin, Claudin1, Zo-1, and Scrib. (*B*) Intestinal sections were stained for Zo-1, and representative images are presented showing decreased Zo-1 after ^{56}Fe radiation. (Scale bars, 5 μm.) (*C*) Intestinal sections were stained for Scrib, and a representative image for each group is presented showing decreased Scrib expression after ^{56}Fe radiation. (Scale bars, 10 μm.) (*D*) Immunoblot analysis of microtubule-associated proteins was performed, and representative images are presented showing radiation-induced altered expression of Tau, phospho-Tau, Crmp2, and Map1b.

migration. So far, our data demonstrate that ^{56}Fe radiation perturbed cytoskeleton, cell adhesion, microtubule, and cell polarity dynamics affecting the rate of the IEC migration along the crypt–villus axis. It is established that multipotent crypt stem cells differentiate into different epithelial cell types, including enterocytes and Paneth cells, and reside in a continuum (24). However, migration of differentiated IECs is not unidirectional and, unlike other upward-migrating differentiated cells, Paneth cells migrate downward to their permanent position at the crypt base (24). To address the question of whether ^{56}Fe radiation apart from decreasing cell migration is affecting direction of migration and cell positioning in the intestinal epithelium, we stained Paneth cells for their marker protein lysozyme using anti-lysozyme antibody in intestinal sections. Our data demonstrate that Paneth cells are residing at the crypt bottom in 7- (*SI Appendix*, Fig. S4*B*, *Upper*) as well as 60- (*SI Appendix*, Fig. S4*B*, *Lower*) d postirradiation samples, suggesting that radiation exposure did not alter cell positioning and direction of migration in the intestinal epithelium.

Increased Integrins and Decreased NH_2-Terminal Fragment of Villin Altered Cell–Substratum Interaction and Cell Extrusion Dynamics in Villi. IEC migration not only involves cell–cell interactions but also involves cell–ECM interactions, and integrins mediating interaction between the ECM and migrating cells (schematically shown in Fig. 5*A*) are dynamic, with attachment and detachment working in tandem to facilitate migration. Since modulation of integrins has been reported to affect IEC migration (25), we assessed levels of two integrins, β1 and β7, using immunofluorescence and immunoblots. Immunofluorescence staining showed higher expression of β1-integrin in intestinal villi 7 (Fig. 5*B* and *SI Appendix*, Fig. S4*C*, *Left*) and 60 (Fig. 5*B* and *SI Appendix*, Fig. S4*C*, *Right*) d after ^{56}Fe relative to control and γ-rays. Furthermore, immunoblot analysis of β1- and β7-integrins also showed higher expression 7 (Fig. 5*C* and *SI Appendix*, Fig. S4*D*, *Left*) and 60 (Fig. 5*C* and *SI Appendix*, Fig. S4*D*, *Right*) d after ^{56}Fe relative to control and γ-rays, suggesting increased cell–ECM attachment promoting reduced cellular mobility. Coordinated cell migration along the crypt–villus axis also requires timely cell extrusion in the villus tip area, and proapoptotic NH_2-terminal villin has been reported to play key roles in cell shedding (18). Immunohistochemistry for NH_2-terminal villin showed reduced expression in the villus tip area at 7 (Fig. 5*D*, *Upper*) and 60 (Fig. 5*D*, *Lower*) d, suggesting decreased shedding of villus tip cells that could potentially contribute to slow cell migration after ^{56}Fe radiation relative to γ-rays.

Cell Proliferation and Migration Factors Are Altered Long-Term After Heavy-Ion Radiation. Although we have shown altered cell proliferation and migration factors up to 60 d after radiation, the key question was to test persistence of these effects long-term. We used 12-mo postirradiation samples to assess selected proliferation and migration factors which are altered at the 7- and 60-d time points. Immunoblots showed increased expression of progrowth β-catenin and its downstream EphB3 but decreased expression of cell adhesion (E-cadherin), cell polarity (Par3), tight junction (Zo-1), and microtubule-associated (Map1b) proteins after ^{56}Fe radiation (Fig. 6*A* and *SI Appendix*, Fig. S5*A*). Heavy-ion ^{56}Fe radiation also increased expression of β1-integrin, suggesting deregulated cell–ECM interaction (Fig. 6*A* and *SI Appendix*, Fig. S5*A*). Immunoblot data were further confirmed by immunofluorescence staining, which showed decreased levels of E-cadherin (Fig. 6*B* and *SI Appendix*, Fig. S5*B*) and Par3 (Fig. 6*C* and *SI Appendix*, Fig. S5*C*) proteins 12 mo after ^{56}Fe radiation, suggesting long-term effects.

Altered Cell Migration Factors Are Associated with Intestinal Metaplasia in Wild-Type C57BL/6J Mice and Intestinal Tumorigenesis in APC$^{1638N/+}$ Mice After ^{56}Fe Radiation. Since the wild-type mice used in the study do not develop GI tumors, we investigated if there is any indication of ^{56}Fe radiation-induced cellular transformation using the intestinal metaplasia marker guanylyl cyclase C (GC-C) (26). Immunohistochemistry for GC-C in wild-type mice showed increased staining after ^{56}Fe radiation relative to control and γ-rays (Fig. 6*D* and *SI Appendix*, Fig. S5*D*). Deregulation of cell migration is linked to intestinal pathologies such as cancer in human (10) as well as in mouse models, such as adenomatous polyposis coli (APC) mutant mouse models (27). APC mutants, such as APC$^{Min/+}$ and APC$^{1638N/+}$, develop intestinal tumors, and we used APC$^{1638N/+}$ mice bearing a truncation mutation in the APC gene in the C57BL/6J background to assess intestinal cell migration perturbations as well as tumorigenesis in the same mice. While we reported increased intestinal tumorigenesis in APC$^{1638N/+}$ mice previously (5), additional data have

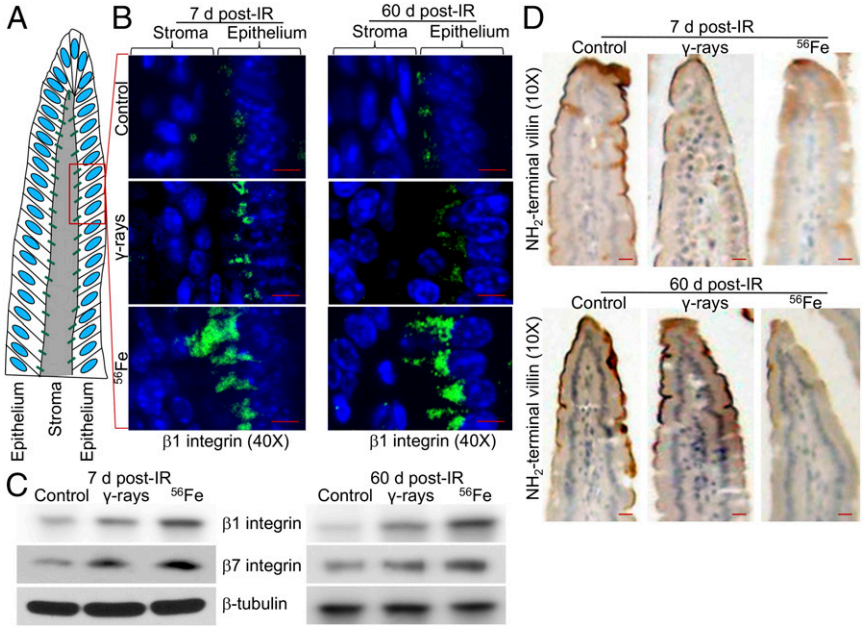

Fig. 5. Persistent deregulation of integrins and NH_2-terminal villin after heavy-ion radiation exposure. (*A*) Schematic representation of integrin (green bars)-mediated interaction between the epithelial cell and stroma in the intestinal villus, and the red box highlights the area presented in the immunofluorescence images. (*B*) Sections were stained for β1-integrin, and representative images are presented showing increased β1-integrin expression after ^{56}Fe radiation. (Scale bars, 5 μm.) (*C*) Immunoblots showing radiation-induced increased expression of β1- and β7-integrins after ^{56}Fe radiation. (*D*) Sections were immunohistochemically stained for NH_2-terminal villin, an intestinal villus tip cell apoptosis marker. Representative images captured at 10× microscopic magnification are presented showing decreased expression of NH_2-terminal villin in areas near the villus tip after ^{56}Fe radiation. (Scale bars, 10 μm.)

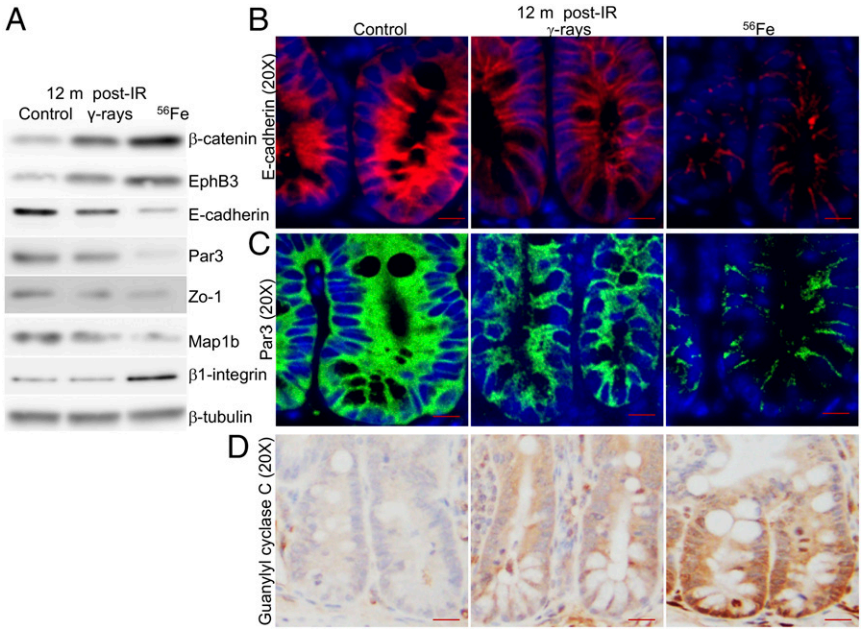

Fig. 6. Long-term up-regulation of proliferative markers and down-regulation of cell migration factors along with increased intestinal metaplasia after ^{56}Fe radiation. (*A*) Representative immunoblot images are presented showing increased β-catenin, EphB3, and β1-integin and decreased expression of E-cadherin, Par3, Zo-1, and Map1b 12 mo after ^{56}Fe radiation. (*B*) E-cadherin expression was assessed by immunofluorescence in intestinal sections, and representative images are presented showing decreased expression after ^{56}Fe radiation. (Scale bars, 10 μm.) (*C*) Representative immunofluorescence images of Par3 from intestinal sections are presented showing decreased expression after ^{56}Fe radiation. (Scale bars, 10 μm.) (*D*) Expression of GC-C, a marker of intestinal metaplasia, is shown in representative images. (Scale bars, 10 μm.)

since been acquired and added to demonstrate a higher tumor frequency after ^{56}Fe relative to control and γ-rays (Fig. 7*A*). Selected cell migration parameters were assessed in the tumor and tumor-adjacent normal intestinal tissues. Immunoblot analysis showed increased EphB3 and decreased Claudin1, Zo-1, and Map1b in normal (Fig. 7*B*, *Left* and *SI Appendix*, Fig. S6*A*) as well as in tumor (Fig. 7*B*, *Right* and *SI Appendix*, Fig. S6*B*) tissues after ^{56}Fe radiation. Immunoblot data also showed increased β1-integrin and align with our data in wild-type mouse cells, suggesting altered cell–ECM interaction in tumor and tumor-adjacent normal tissues after ^{56}Fe radiation. Immunofluorescence staining was performed and analyzed showing decreased polarity protein Par3 (Fig. 7*C* and *SI Appendix*, Fig. S6*C*) and cell adhesion protein E-cadherin (Fig. 7*D* and *SI Appendix*, Fig. S6*D*) in normal and tumor tissues, supporting the immunoblot data. Since cellular proliferation and differentiation are intimately linked to both tumorigenesis and cell migration, we stained intestinal sections for CyclinD1, which is a proliferation marker and a β-catenin target gene and scored positive nuclei in tumor and normal tissues. Increased CyclinD1 was observed in both normal and tumor tissues after ^{56}Fe radiation (Fig. 7*E*). Goblet cells are one of the differentiated cell types in the intestinal epithelium, and Alcian blue staining showed decreased staining, suggesting reduced differentiation after ^{56}Fe radiation in normal (Fig. 7*F* and *SI Appendix*, Fig. S6*E*) as well as in tumor (Fig. 7*G* and *SI Appendix*, Fig. S6*F*) tissues. Overall, cell migration data in tumor and adjacent normal tissue correlate not only with tumorigenesis in APC$^{1638N/+}$ but also with data in wild-type mice.

Heavy-Ion Radiation Compromised Intestinal Brush Border Enzymes, Membrane Transport, and Barrier Function in Wild-Type Mice 12 Mo After Exposure. Coordinated and timely cell turnover is essential for nutrient absorption and barrier function, which are key functionalities of intestinal epithelial cells. Radiation has been reported to affect both nutrient absorption and barrier function at relatively high doses (20, 28). Here we assessed intestinal epithelial cell functions using activity assays, qRT-PCR (quantitative real-time PCR), and ELISA at a low dose of radiation. Measuring gamma-glutamyl transferase (GGT), invertase, and intestinal alkaline phosphatase (ALP) activities in intestinal tissue 12 mo after radiation showed increased GGT, unchanged invertase, and decreased ALP (*SI Appendix*, Fig. S7*A*) with implications for protein, carbohydrate, and fat absorption, respectively. Various transporters on intestinal epithelial cells play key roles in nutrient absorption, and expression of a chosen panel of transporter genes encompassing key nutrients such as carbohydrates and fatty acids was examined in intestinal tissue by qRT-PCR showing differential alterations 12 mo after γ- and ^{56}Fe radiation (*SI Appendix*, Fig. S7*B* and Tables S4 and S5). Changes in circulating citrulline and intestinal fatty acid-binding protein (I-FABP) levels have been established as useful serum markers for assessing mucosal barrier function (29). Serum citrulline and I-FABP measured by ELISA in 12-mo samples showed decreased citrulline levels (*SI Appendix*, Fig. S7*C*) and increased I-FABP levels (*SI Appendix*, Fig. S7*C*) after ^{56}Fe radiation exposure, suggesting altered intestinal mucosal integrity.

Low-Dose ^{56}Fe Radiation Exposure Is Associated with Persistently Increased DNA Damage. Radiation exposure is associated with DNA damage, and ^{56}Fe due to its high-LET characteristic is known to induce greater DNA damage relative to low-LET γ-radiation (4). Intestinal sections from 7-d, 60-d, and 12-mo postirradiation mice were immunofluorescently stained for γH2AX, and foci were counted and plotted showing persistently higher numbers of foci, suggesting continued DNA double-strand break (DSB) generation after ^{56}Fe relative to control and γ-rays (Fig. 8 *A* and *B* and *SI Appendix*, Fig. S8*A*). We also stained 60-d postexposure samples for 8-oxo-dG, a marker of oxidative DNA damage, and showed higher staining in ^{56}Fe-irradiated samples relative to control and γ-rays (*SI Appendix*, Fig. S8*B*). Since DNA damage is linked to apoptosis, we probed intestinal sections for cell death using the TUNEL assay. Our data showed that the numbers of TUNEL-positive cells in crypts are similar in irradiated and control samples, suggesting that radiation-induced DNA damage is below the apoptotic threshold at the dose tested (*SI Appendix*, Fig. S8*C*).

Since oxidative stress and DNA damage did not increase cell death and sublethal levels of reactive oxygen species are known to propagate proliferative signals, we assessed cell proliferation. Staining for the proliferative marker PCNA showed a higher number of positively stained nuclei, suggesting increased proliferation in 7- and 60-d as well as in 12-mo post–^{56}Fe-irradiated samples relative to control and γ-rays (*SI Appendix*, Fig. S9*A*). To understand the long-term fate of the proliferating cells, we used H&E-stained intestinal sections to count the number of crypts per intestinal section circumference in 60-d and 12-mo samples after sham, γ-, and ^{56}Fe radiation. Results demonstrated significantly

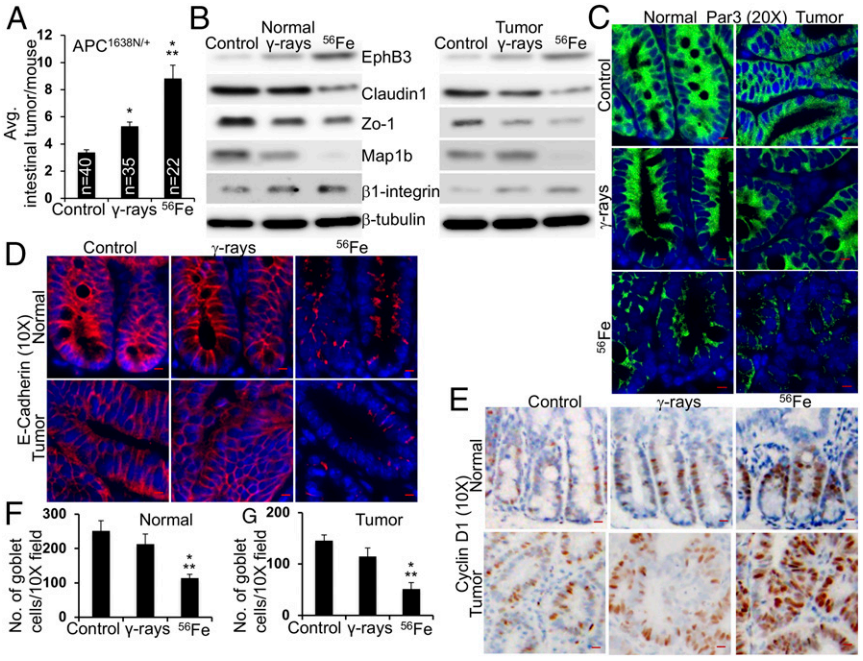

Fig. 7. Altered cell migration factors and increased intestinal tumorigenesis in APC$^{1638N/+}$ mice. (*A*) Increased intestinal tumor frequency is presented graphically showing higher tumorigenesis after ^{56}Fe relative to sham and γ-radiation. (*B*) Immunoblot images showing increased EphB3 and β1-integrin expression and decreased Claudin1, Zo-1, and Map1b expression in tumor and adjacent normal tissues from APC$^{1638N/+}$ mice. (*C*) Representative images of Par3 showing decreased expression in normal and tumor tissues after ^{56}Fe radiation. (Scale bars, 10 μm.) (*D*) Immunofluorescence images showing decreased expression of E-cadherin in normal and tumor tissues after ^{56}Fe radiation. (Scale bars, 10 μm.) (*E*) Representative images showing increased expression of Cyclin D1 in both normal and tumor tissues after ^{56}Fe radiation. (Scale bars, 10 μm.) (*F* and *G*) Intestinal sections were stained using Alcian blue to score for mucin-producing goblet cells, a differentiated cell type in intestine, in normal and tumor tissues, and results are presented graphically showing decreased number after ^{56}Fe radiation; *, significant relative to control; **, significant relative to γ-rays. Statistical significance is set at $P < 0.05$ and error bars represent mean ± SEM.

higher numbers of crypts per intestinal section of ^{56}Fe-irradiated samples relative to control and γ-rays (*SI Appendix*, Fig. S9*B*), suggesting persistent accumulation of proliferating cells in the crypt area.

Persistent Senescence and Senescence-Associated Secretory Phenotype in Intestinal Epithelial Cells After ^{56}Fe Radiation. Since DNA damage is known to trigger cellular senescence (30), we stained frozen intestinal sections from 7-d, 60-d, and 12-mo postirradiated mice for senescence-associated β-galactosidase (SA-β-gal), a known marker of senescence. SA-β-gal–positive cells were counted at three time points showing progressively increased senescence over time (Fig. 8 *C* and *D* and *SI Appendix*, Fig. S10), which is congruent with persistent γH2AX count. Expression analysis of additional senescent markers, p16 and p21, was performed by qRT-PCR and both showed increased expression after ^{56}Fe radiation (Fig. 8*E* and *SI Appendix*, Tables S4 and S6), supporting the SA-β-gal data. We hypothesized that acquisition of the secretory phenotype (SASP) by DNA damage-induced senescent cells is providing an impetus to deregulate cellular processes involved in cell migration. To this end, we costained intestinal sections with a senescent marker (Glb1) and a SASP marker (IL8) that showed increased SASP cells after ^{56}Fe radiation (Fig. 8*F*). Quantification of SASP cells showed a significantly higher number of IL8-positive senescent (Glb1-positive) cells in ^{56}Fe samples relative to control and γ-rays (Fig. 8*G*). We used qRT-PCR to assess expression of a panel of SASP genes and showed up-regulation of *IL6*, *Ptges*, *Faim2*, and *Opg* (Fig. 8*H* and *SI Appendix*, Table S6), supporting immunofluorescence data.

Discussion

Epithelial cell turnover is important for maintaining overall GI health, and its perturbation by space radiation, as well as by heavy-ion radiotherapy, raises concerns that require an understanding of its molecular underpinnings. Using the small intestine with its crypt–villus axis as a model system, we show in WT mice that heavy ions negatively impact cell migration as well as molecular events associated with it up to 12 mo later; an overview of our results is included in *SI Appendix*, Table S7. While a smaller, modest effect was seen early (7 d) after the same dose of γ-rays, cell migration recovered to normal later (60 d), and effects of heavy ions on cell migration were more pronounced relative to γ-rays. Importantly, our data in APC$^{1638N/+}$ mice demonstrate decreased cell migration signaling is concomitant with increased intestinal tumorigenesis. Hallmarks of increased cell senescence and the SASP were seen in crypt regions after heavy ions, including increased SA-β-gal and IL8 along with an ongoing DNA damage response (DDR), as exemplified by increased γH2AX foci; remarkably, these persisted for a year after irradiation, and actually increased with time. This was accompanied by an increased proliferative response and β-catenin activation, and also changes in intestinal nutrient absorption and barrier function factors. Overall, our results support the conclusion that even low-dose heavy-ion radiation triggers persistent stress signaling and the SASP with adverse changes in the intestine.

The canonical Wnt pathway along with its central signal transducer, β-catenin, is involved in maintaining intestinal homeostasis (31). Our data demonstrate persistent up-regulation of not only β-catenin but also phospho-GSK3β, which inactivates GSK3β and scuttles β-catenin degradation, after heavy-ion radiation. Wnt signaling is fine-tuned with coordination between several agonist and antagonists, and Dkk1, a Wnt antagonist, blocks canonical Wnt signaling (13). Here we show that ^{56}Fe radiation even after 60 d depleted Dkk1 expression in mouse intestine, which could further explain radiation-induced β-catenin up-regulation. Escape of β-catenin from degradation allows its cytoplasmic accumulation and subsequent nuclear translocation for transcriptional activation

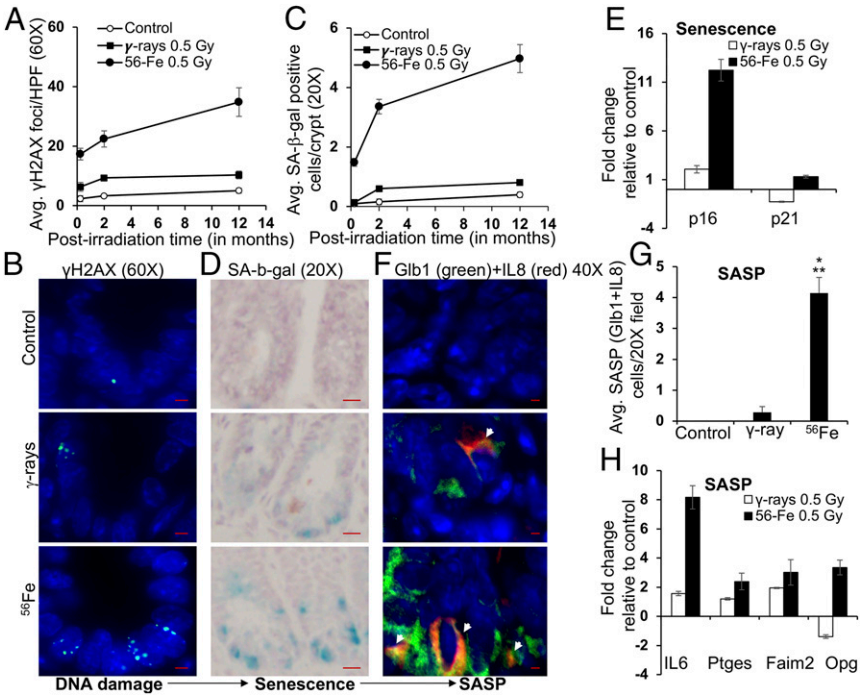

Fig. 8. Ongoing DNA damage, induction of cellular senescence, and acquisition of the senescence-associated secretory phenotype 12 mo after ^{56}Fe radiation. (*A* and *B*) γH2AX foci counts are graphically plotted demonstrating long-term persistence of DNA damage after ^{56}Fe relative to γ-rays and control. Representative images from 12-mo samples showing increased DNA double-strand breakage after ^{56}Fe radiation. HPF, high-power field. (Scale bars, 5 μm.) (*C* and *D*) Numbers of SA-β-gal–positive cells are plotted graphically showing persistently higher senescence induction after ^{56}Fe radiation. (Scale bars, 10 μm.) (*E*) Quantitative RT-PCR results show increased expression of p16 and p21 after ^{56}Fe radiation. (*F*) Representative costaining images showing Glb1+IL8–positive cells (white arrowheads) in ^{56}Fe samples. (Scale bars, 5 μm.) (*G*) Quantification of Glb1+IL8 cells per 20× field is presented graphically showing higher numbers in ^{56}Fe relative to control and γ-rays. (*H*) Quantitative RT-PCR results showing increased expression of *IL6*, *Ptges*, *Faim2*, and *Opg* after ^{56}Fe radiation; *, significant relative to control; **, significant relative to γ-rays. Statistical significance is set at $P < 0.05$ and error bars represent mean ± SEM.

of responsive genes such as EphB3 and EphrinB1 (12). Our data show that EphrinB1 and EphrinB2 ligands and their EphB2 and EphB3 receptors are persistently up-regulated, and such events could affect IEC migration. We next queried whether heavy-ion radiation exposure is modulating β-catenin/TCF4 binding to *EphrinB* and *EphB* promoters. ChIP analysis data demonstrate enhanced recruitment of β-catenin/TCF4 to the *EphB3* and *EphrinB1* promoters after ^{56}Fe radiation, and could be due to radiation-induced up-regulation of β-catenin. A spatial gradient of EphrinB/EphB along the crypt–villus axis determines the directional migration of IECs (32), and our Paneth cell staining data demonstrate that heavy-ion radiation did not alter the direction of migration, which could be due to up-regulation of both the receptors, EphB2 and EphB3, and the ligands, EphrinB1 and EphrinB2.

The observed effects of increased accumulation of β-catenin and consequent up-regulation of β-catenin target genes have two general implications: first, progrowth oncogenic stress, and second, cytoskeletal dynamics perturbations; both are expected to adversely impact coordinated IEC migration. Increased expression of proproliferative oncogenes such as β-catenin leads to oncogenic stress that has been reported to induce DNA DSBs via DNA replication fork collapse-mediated replication stress (33). Oncogenic stress is interlinked with oxidative stress (33), and our current data showing increased β-catenin, DNA damage, and oxidative stress are consistent with our previous data showing persistent stress after heavy-ion radiation exposure (4). However, despite increased cellular stress, we did not observe any alteration in cell death, suggesting persistent levels of DNA damage below the apoptotic threshold, which is also consistent with our previous observations (4). Furthermore, our data support the notion that cells are proliferating in the presence of sublethal DNA damage and oxidative stress and that growing cells are accumulating in the crypt area, as evidenced by increased crypt numbers after heavy-ion radiation. It is reasonable to assume that increased β-catenin and decreased E-cadherin are altering β-catenin/E-cadherin dynamics (34), which work in tandem to affect cell–cell adhesion and thus cell migration after heavy-ion radiation. We further hypothesize that heavy-ion radiation-induced increased β-catenin and DNA damage must be altering cytoskeleton dynamics through modulation of cell–cell and cell–ECM interactions, cell polarity and positioning, and microtubule turnover and cell shedding to deregulate IEC migration (12). Cellular apicobasal polarity is established and regulated via Par3/Par6/PKC/Cdc42 complex formation (35), and our data show that the polarity-associated molecule Par3 is down-regulated after ^{56}Fe radiation. Additionally, Cdc42 is known to regulate actin dynamics, especially actin microspike formation, and thus be influencing cell polarity and morphology (36). Therefore, heavy-ion radiation-induced decreased expression of Cdc42 along with Par3 probably contributes to altered cell polarity dynamics and thus deregulated cell migration.

Cellular tight junction is regulated through Claudin1, Occludin, and the junctional adhesion molecule family of proteins. We found that ^{56}Fe radiation down-regulated expression of Zo-1, Claudin1, and Scribe in mouse intestine, and such down-regulation could have contributed to perturbation of collective cell migration. This agrees with the recent report showing high-dose γ-radiation inhibits the expression of Zo-1, Claudin3, and E-cadherin, disrupting tight junctions, adherens junctions, and actin cytoskeleton dynamics by an oxidative stress-dependent mechanism in mouse intestine (37). Cell adhesion and microtubule dynamics are also regulated by Rock1 and Mlck through phosphorylation of myosin regulatory light chain-mediated changes in actomyosin contractility (36). In our study, increased Rock1 and decreased Mlck are expected to further destabilize cytoskeletal dynamics and thus disturb coordinated cell migration. Microtubules play a critical role in cytoskeleton remodeling during cell migration. Our data on Map1b and Tau, which mediate interaction between microtubule and other cytoskeleton elements for coordinated cell migration, suggest that heavy-ion radiation exposure compromises microtubule dynamics. Additionally, dynamic interactions between cells' cytoskeleton and ECM through integrins are also essential for coordinated cellular movement (38). We have shown that ^{56}Fe radiation exposure was associated with increased expression of two integrins that could contribute to decreased dynamicity between cell and ECM, ultimately contributing to persistently slower migration after heavy ions relative to γ-rays and control samples. It is also important that migrating cells upon reaching the villus tip are shed via apoptosis in a timely manner to make way for the incoming new cells (17). Our data on down-regulation of proapoptotic NH_2-terminal villin at the villus tip are suggestive of compromised cell shedding along with decreased

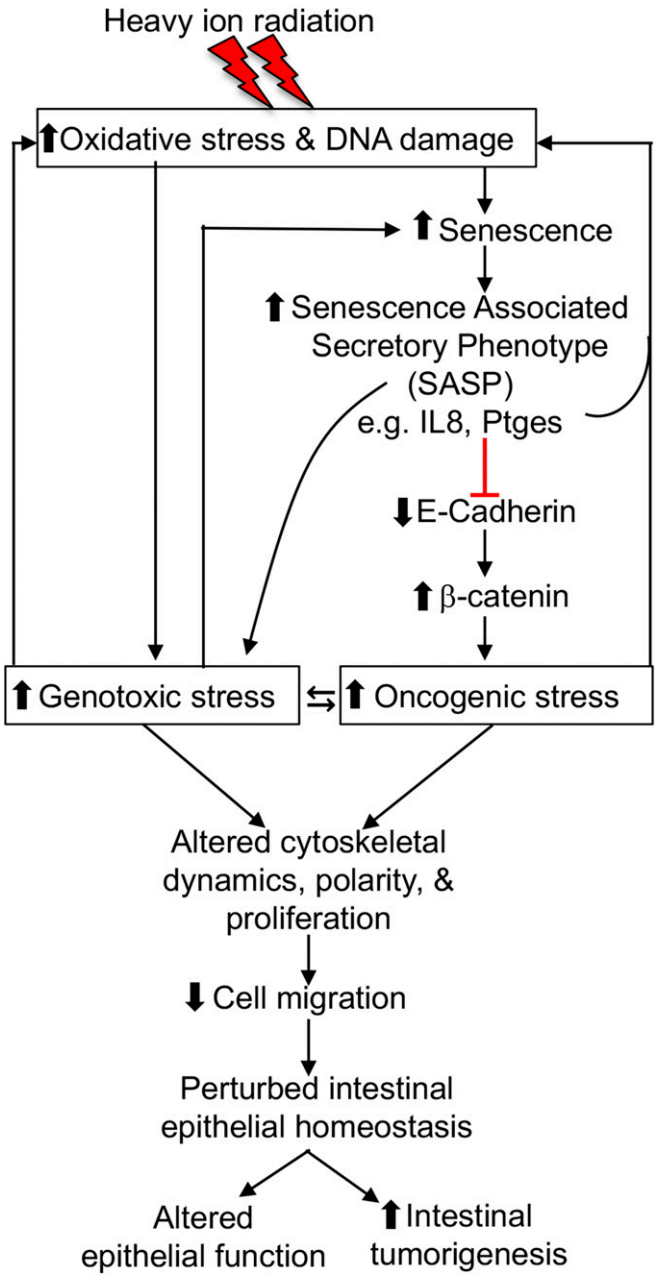

Fig. 9. Proposed model for altered IEC migration and pathophysiology after heavy-ion space radiation. Unlike low-LET γ-radiation, ^{56}Fe ions trigger long-term perturbation in IECs, including direct damage with the generation of senescent cells and long-term signaling abnormalities consistent with SASP responses. Ongoing oxidative stress can further exacerbate signaling events affecting proliferation and differentiation, cell–cell interactions, cell–ECM interaction, as well as generation of additional senescent cells. The presence of senescent cells in crypts indicates that these events impact stem cell function.

migration after heavy ions, which further highlights the broad impact of heavy ions on normal intestinal homeostasis.

Altered migration of intestinal epithelial cells could not only compromise barrier function and nutrient absorption but could also prolong exposure of cells to luminal content and initiate stress responses with pathological consequences, including colon cancer (10). Increased DNA damage evidenced by increased 8-oxo-dG and γH2AX observed in our study could be due to decreased migration allowing increased cell luminal content contact time. DNA damage in our study progressively increased and persisted 12 mo after radiation exposure, and persistent DNA damage can be a trigger for cellular senescence (30) as well as a reflection of increased senescent cells. Indeed, the increasing number of senescent cells observed 12 mo after heavy-ion radiation correlates with persistent γH2AX foci count. Since a primary heavy-ion ^{56}Fe radiation track hit to a cell is expected to induce irreversible damage, it is possible that initial sublethal DNA damage is induced either by secondary delta rays or by non-targeted effects, allowing intestinal stem cells to survive and propagate effects long-term (39). The initial DNA damage could also stochastically induce senescence, which also allows cells to survive without propagation but with SASP potential. Indeed, some of the senescent cells costained with IL8, indicating acquisition of the SASP, and our data align with earlier reports on radiation-induced SASP (30). Our results show altered activity of GGT and ALP involved in amino acid and fat absorption (40) as well as decreased expression of glucose, cholesterol, and fatty acid transporters and intestinal hormones, supporting the notion that heavy-ion radiation-induced decreased cell migration is affecting intestinal function. I-FABP and citrulline are produced by intestinal epithelial cells, and their serum levels have been reported as an indicator of intestinal epithelial integrity (29). Our results showing increased I-FABP and decreased citrulline suggest compromised epithelial integrity, which could be due to either a SASP-mediated chronic inflammatory stress or changes in microbiota, and is in agreement with previous observations (29). While we previously reported compromised barrier function and altered intestinal epithelial morphology, albeit at higher doses (20), the current study not only shows loss of epithelial function but also initiation of pathological processes evidenced by increased intestinal metaplasia marker at a low dose of heavy ions. Although WT mice show metaplasia, they are resistant to spontaneous intestinal tumor development, and therefore we used $APC^{1638N/+}$ mice to demonstrate concurrently decreased migration signaling molecules and increased intestinal tumorigenesis. Evidence in the literature (27) along with our $APC^{1638N/+}$ data led us to conclude that slow cell migration is contributing to intestinal tumor initiation and promotion after heavy-ion radiation exposure.

In summary, our findings provide experimental evidence unraveling the molecular underpinnings of how high-LET heavy-ion radiation in contrast to low-LET γ-rays can deregulate IEC migration even at a low dose. Although we used the small intestine as a model to study heavy-ion radiation effects on cell migration, our observations could have wider applicability for other GI sites including the colon, which is prone to carcinogenesis. Overall, our analysis provides insight into the effects of heavy-ion radiation on molecular events involved in IEC migration including (*i*) cell proliferation, (*ii*) cell–cell interaction, (*iii*) cell–ECM interaction, and (*iv*) cell shedding. It is conceivable that chronic Wnt/β-catenin activation and oxidative stress are the two central events cooperatively working to modulate cell migration dynamics after heavy-ion radiation exposure. Given that β-catenin triggers proliferation and oxidative stress triggers the DDR, an appealing probability is that a combination of proliferative and DDR signals could be slowing down cell migration through initial generation of senescent cells by densely ionizing heavy ions, and then a feedback loop involving ongoing generation of additional senescent cells by SASP signaling and ongoing DNA damage and resultant DDR. A key question that future studies will need to address is the role of intestinal stem cells in heavy-ion radiation-induced DNA damage, senescence, SASP, deregulated cell migration, and risk of GI pathologies. We propose that persistent genotoxic and oncogenic stress is triggering cellular senescence, with some of the senescent cells acquiring the SASP with secretion of proinflammatory factors leading to intestinal pathophysiological changes (Fig. 9). We may consider whether modulation of β-catenin activity, oxidative stress, and/or SASP could be advantageous in mitigating some of the risk of heavy-ion radiation-induced GI pathology for astronauts and radiotherapy patients.

Materials and Methods

Mouse Irradiation. Wild-type mice (C57BL/6J; male, 6 to 8 wk old; $n = 10$) were irradiated (dose: 0.5 Gy) using a simulated space radiation source at the NASA Space Radiation Laboratory (NSRL), Brookhaven National Laboratory for iron (^{56}Fe; energy: 1,000 MeV per nucleon; LET: 148 keV/μm) irradiation, and a ^{137}Cs source was used for γ-ray (LET: 0.8 keV/μm) whole-body irradiation of mice. Mice were euthanized either 7 d, 60 d, or 12 mo after radiation exposure. For BrdU pulse labeling, mice were intraperitoneally administered 30 mg/kg BrdU 24 h before euthanasia. Since wild-type C57BL/6J mice are resistant to tumor development, we also exposed APC$^{1638N/+}$ mice to the same dose of γ- and ^{56}Fe radiation detailed above to correlate effects on intestinal cell migration parameters with tumorigenesis after exposure to different radiation types. As described previously (5), APC$^{1638N/+}$ mice were euthanized 150 d after radiation exposure. All animal procedures were performed as per protocols approved by the Institutional Animal Care and Use Committee at Brookhaven National Laboratory (Protocol#345) and at Georgetown University (Protocol#2016-1129). Our study followed the *Guide for the Care and Use of Laboratory Animals* (41). Additional detail about animal care is provided in *SI Appendix*, Section *H*.

Sample Collection, Histology, and Immunostaining. In WT mice, intestinal tissues from the jejunal–ilial junction were surgically removed from euthanized mice and flush-cleaned using PBS. In APC$^{1638N/+}$ mice, intestinal tumors were counted as described previously (5) and tumor and tumor-adjacent normal tissues were collected for further analysis. Tissues were fixed in 10% buffered formalin, paraffin-embedded, and sectioned at 5-μm thickness for hematoxylin and eosin (H&E) staining and immunostaining. Sections were deparaffinized, sequentially rehydrated, and H&E-stained using established procedures. For 8-oxo-dG and BrdU staining, rehydrated sections were treated with 2 M HCl for 20 min at 37 °C followed by neutralization with 0.1 M borate buffer for 10 min at room temperature (RT) and incubated overnight with either anti–8-oxo-dG or anti-BrdU antibodies at 4 °C. For immunostaining of other proteins, rehydrated sections were used for antigen retrieval in pH 6.0 citrate buffer (Dako) for 20 min. All sections were permeabilized in 0.3% Triton X-100 and blocked with 5% BSA at RT followed by incubation in specific primary antibody at 4 °C. Detail about the immunostaining procedure is provided in *SI Appendix*, Section *H*.

Assessing IEC Migration. Sections stained with anti-BrdU antibody were scored for measuring IEC migration distance along the crypt–villus axis using a method described previously (27). Briefly, in each crypt–villus unit, we marked the highest BrdU-labeled cell and counted the number of cells between the highest-labeled cell and the lowest cell in the crypt. We counted 10 crypt–villus units in each mouse, and 10 different mice were used in each study group for 7- and 60-d time points. IEC migration measured in cell distance after irradiation is presented as percent change in migration distance relative to control (100%) per villus–crypt unit per mouse.

Additional Methods, Image Analysis, and Statistical Consideration. Methods describing immunoblots, nutrient absorption and barrier function measurement, qRT-PCR for nutrient absorption, senescence, and senescence-associated secretory phenotype gene expression analysis, TUNEL assay, ChIP real-time PCR, Alcian blue staining, Cdc42 activity assay, SA-β-gal staining, tumor frequency count, and statistical analysis are provided in *SI Appendix*, Sections *D–H*. Statistical significance is set at $P < 0.05$ and error bars represent mean ± SEM.

ACKNOWLEDGMENTS. We are thankful to the NSRL, especially Drs. Peter Guida and Adam Rusek, for their excellent support. This study is funded through NASA Grants NNX13AD58G and NNX15AI21G. The Histopathology and Tissue Shared Resource is partially supported by NIH/National Cancer Institute (NCI) Grant P30-CA051008.

1. Dupree-Ellis E, Watkins J, Ingle JN, Phillips J (2000) External radiation exposure and mortality in a cohort of uranium processing workers. *Am J Epidemiol* 152:91–95.
2. Preston DL, et al. (2007) Solid cancer incidence in atomic bomb survivors: 1958–1998. *Radiat Res* 168:1–64.
3. Thompson DE, et al. (1994) Cancer incidence in atomic bomb survivors. Part II: Solid tumors, 1958–1987. *Radiat Res* 137(Suppl 2):S17–S67, and erratum (1994) 139:129.
4. Datta K, Suman S, Kallakury BV, Fornace AJJ, Jr (2012) Exposure to heavy ion radiation induces persistent oxidative stress in mouse intestine. *PLoS One* 7:e42224.
5. Suman S, et al. (2016) Relative biological effectiveness of energetic heavy ions for intestinal tumorigenesis shows male preponderance and radiation type and energy dependence in APC(1638N/+) mice. *Int J Radiat Oncol Biol Phys* 95:131–138.
6. Curtis SB, Letaw JR (1989) Galactic cosmic rays and cell-hit frequencies outside the magnetosphere. *Adv Space Res* 9:293–298.
7. Hayatsu K, et al. (2009) HZE particle and neutron dosages from cosmic rays on the lunar surface. *J Phys Soc Jpn* 78:149–152.
8. Kamada T, et al. (2015) Carbon ion radiotherapy in Japan: An assessment of 20 years of clinical experience. *Lancet Oncol* 16:e93–e100.
9. Wong MH, Hermiston ML, Syder AJ, Gordon JI (1996) Forced expression of the tumor suppressor adenomatosis polyposis coli protein induces disordered cell migration in the intestinal epithelium. *Proc Natl Acad Sci USA* 93:9588–9593.
10. Peterson LW, Artis D (2014) Intestinal epithelial cells: Regulators of barrier function and immune homeostasis. *Nat Rev Immunol* 14:141–153.
11. Meineke FA, Potten CS, Loeffler M (2001) Cell migration and organization in the intestinal crypt using a lattice-free model. *Cell Prolif* 34:253–266.
12. Clevers H, Batlle E (2006) EphB/EphrinB receptors and Wnt signaling in colorectal cancer. *Cancer Res* 66:2–5.
13. Koch S, et al. (2009) Dkk-1 inhibits intestinal epithelial cell migration by attenuating directional polarization of leading edge cells. *Mol Biol Cell* 20:4816–4825.
14. Zhang DY, Wang HJ, Tan YZ (2011) Wnt/β-catenin signaling induces the aging of mesenchymal stem cells through the DNA damage response and the p53/p21 pathway. *PLoS One* 6:e21397.
15. Liu YT, et al. (2007) Chronic oxidative stress causes amplification and overexpression of ptprz1 protein tyrosine phosphatase to activate beta-catenin pathway. *Am J Pathol* 171:1978–1988.
16. Hall AE, et al. (2016) The cytoskeleton adaptor protein ankyrin-1 is upregulated by p53 following DNA damage and alters cell migration. *Cell Death Dis* 7:e2184.
17. Patterson AM, Watson AJM (2017) Deciphering the complex signaling systems that regulate intestinal epithelial cell death processes and shedding. *Front Immunol* 8:841.
18. Wang Y, et al. (2016) Both the anti- and pro-apoptotic functions of villin regulate cell turnover and intestinal homeostasis. *Sci Rep* 6:35491.
19. Suman S, Kallakury BV, Fornace AJJ, Jr, Datta K (2015) Protracted upregulation of leptin and IGF1 is associated with activation of PI3K/Akt and JAK2 pathway in mouse intestine after ionizing radiation exposure. *Int J Biol Sci* 11:274–283.
20. Datta K, et al. (2012) Accelerated hematopoietic toxicity by high energy (56)Fe radiation. *Int J Radiat Biol* 88:213–222.
21. Cucinotta FA, Durante M (2006) Cancer risk from exposure to galactic cosmic rays: Implications for space exploration by human beings. *Lancet Oncol* 7:431–435.
22. Hassler DM, et al.; MSL Science Team (2014) Mars' surface radiation environment measured with the Mars Science Laboratory's Curiosity rover. *Science* 343:1244797.
23. Fukata Y, et al. (2002) CRMP-2 binds to tubulin heterodimers to promote microtubule assembly. *Nat Cell Biol* 4:583–591.
24. Barker N, van de Wetering M, Clevers H (2008) The intestinal stem cell. *Genes Dev* 22:1856–1864.
25. Kaemmerer E, et al. (2015) Beta-7 integrin controls enterocyte migration in the small intestine. *World J Gastroenterol* 21:1759–1764.
26. Birbe R, et al. (2005) Guanylyl cyclase C is a marker of intestinal metaplasia, dysplasia, and adenocarcinoma of the gastrointestinal tract. *Hum Pathol* 36:170–179.
27. Javid SH, Moran AE, Carothers AM, Redston M, Bertagnolli MM (2005) Modulation of tumor formation and intestinal cell migration by estrogens in the Apc(Min/+) mouse model of colorectal cancer. *Carcinogenesis* 26:587–595.
28. Lutgens L, Lambin P (2007) Biomarkers for radiation-induced small bowel epithelial damage: An emerging role for plasma citrulline. *World J Gastroenterol* 13:3033–3042.
29. Wells JM, et al. (2017) Homeostasis of the gut barrier and potential biomarkers. *Am J Physiol Gastrointest Liver Physiol* 312:G171–G193.
30. Kim SB, et al. (2016) Radiation promotes colorectal cancer initiation and progression by inducing senescence-associated inflammatory responses. *Oncogene* 35:3365–3375.
31. Fevr T, Robine S, Louvard D, Huelsken J (2007) Wnt/beta-catenin is essential for intestinal homeostasis and maintenance of intestinal stem cells. *Mol Cell Biol* 27:7551–7559.
32. Batlle E, et al. (2002) Beta-catenin and TCF mediate cell positioning in the intestinal epithelium by controlling the expression of EphB/EphrinB. *Cell* 111:251–263.
33. Mallette FA, Ferbeyre G (2007) The DNA damage signaling pathway connects oncogenic stress to cellular senescence. *Cell Cycle* 6:1831–1836.
34. Nelson WJ, Nusse R (2004) Convergence of Wnt, beta-catenin, and cadherin pathways. *Science* 303:1483–1487.
35. Joberty G, Petersen C, Gao L, Macara IG (2000) The cell-polarity protein Par6 links Par3 and atypical protein kinase C to Cdc42. *Nat Cell Biol* 2:531–539.
36. Citalán-Madrid AF, García-Ponce A, Vargas-Robles H, Betanzos A, Schnoor M (2013) Small GTPases of the Ras superfamily regulate intestinal epithelial homeostasis and barrier function via common and unique mechanisms. *Tissue Barriers* 1:e26938.
37. Shukla PK, et al. (2016) Rapid disruption of intestinal epithelial tight junction and barrier dysfunction by ionizing radiation in mouse colon in vivo: Protection by *N*-acetyl-l-cysteine. *Am J Physiol Gastrointest Liver Physiol* 310:G705–G715.
38. Huttenlocher A, Horwitz AR (2011) Integrins in cell migration. *Cold Spring Harb Perspect Biol* 3:a005074.
39. Buonanno M, de Toledo SM, Pain D, Azzam EI (2011) Long-term consequences of radiation-induced bystander effects depend on radiation quality and dose and correlate with oxidative stress. *Radiat Res* 175:405–415.
40. Hauge T, Nilsson A, Persson J, Hultberg B (1998) Gamma-glutamyl transferase, intestinal alkaline phosphatase and beta-hexosaminidase activity in duodenal biopsies from chronic alcoholics. *Hepatogastroenterology* 45:985–989.
41. National Research Council (2011) Guide for the Care and Use of Laboratory Animals (National Academies Press, Washington, DC), 8th Ed.